Immunity, Vol. 18, 301–312, February, 2003, Copyright ©2003 by Cell Press

Regulation of Marginal Zone B Cell Development by MINT, a Suppressor of Notch/RBP-J Signaling Pathway

Kazuki Kuroda,[1,4] Hua Han,[1,4] Shoichi Tani,[1] Kenji Tanigaki,[1] Tin Tun,[1] Takahisa Furukawa,[1] Yoshihito Taniguchi,[1] Hisanori Kurooka,[1] Yoshio Hamada,[3] Shinya Toyokuni,[2] and Tasuku Honjo[1,*]

[1]Department of Medical Chemistry
[2]Department of Pathology and Biology of Diseases
Graduate School of Medicine
Kyoto University
Yoshida-Konoe, Sakyo-ku
Kyoto 606-8501
[3]National Institute for Basic Biology
Okazaki
Aichi 444-8585
Japan

Summary

We found that Msx2-interacting nuclear target protein (MINT) competed with the intracellular region of Notch for binding to a DNA binding protein RBP-J and suppressed the transactivation activity of Notch signaling. Although MINT null mutant mice were embryonic lethal, MINT-deficient splenic B cells differentiated about three times more efficiently into marginal zone B cells with a concomitant reduction of follicular B cells. MINT is expressed in a cell-specific manner: high in follicular B cells and low in marginal zone B cells. Since Notch signaling directs differentiation of marginal zone B lymphocytes and suppresses that of follicular B lymphocytes in mouse spleen, the results indicate that high levels of MINT negatively regulate Notch signaling and block differentiation of precursor B cells into marginal zone B cells. MINT may serve as a functional homolog of *Drosophila* Hairless.

Introduction

The Notch signaling pathway plays a critical role in cell fate determination of various lineages in vertebrates as well as invertebrates (reviewed in Artavanis-Tsakonas et al., 1995, 1999). In *Drosophila* Notch is typically involved in binary cell fate decision at a variety of stages and processes including neurogenesis, myogenesis, and oogenesis. In mammals, Notch regulates development of hematopoietic cells (reviewed in Izon et al., 2002), nervous systems (reviewed in Beatus and Lendahl, 1998), muscle (Kopan et al., 1994; Kuroda et al., 1999), pancreas (Apelqvist et al., 1999), and many other tissues. The Notch signaling appears to exert two opposing functions, namely, facilitation and suppression of differentiation at different stages and lineages. For example, the Notch signaling facilitates differentiation of T lymphocytes from common lymphoid progenitors in thymus while it suppresses differentiation of B lymphocytes in the bone marrow (Han et al., 2002; Radtke et al., 2000). Similarly, Notch signaling regulates the final differentiation step of bone marrow-derived B cells in spleen where the newly formed (or T1) B cells with IgM^{hi} IgD^{lo} $CD21^{lo}$ markers are believed to pass through transitional (or T2) B cells with IgM^{hi} IgD^{hi} $CD21^{int}$ $CD23^{hi}$ markers and then to differentiate into Fo B cells (IgM^{lo} IgD^{hi} $CD21^{int}$ $CD23^{hi}$) or MZ B cells (IgM^{hi} IgD^{lo} $CD21^{hi}$ $CD23^{lo}$) (Martin and Kearney, 2001; Oliver et al., 1997). We recently found that Notch signaling facilitates generation of marginal zone (MZ) B cells while it suppresses generation of follicular (Fo) B cells in spleen (Tanigaki et al., 2002).

The mouse Notch (mNotch) receptor is a large transmembrane protein that is cleaved in the transmembrane region by an unknown presenilin-like protease upon interaction with its ligands, Delta or Jagged/Serrate (Mumm et al., 2000). The intracellular region of mNotch (RAMIC) released by the ligand-induced cleavage directly translocates to the nucleus (Jarriault et al., 1995; Schroeter et al., 1998; Struhl and Adachi, 1998). RAMIC interacts with a DNA binding protein RBP-J (the mammalian homolog of *Drosophila* Suppresser of Hairless [*Su(H)*]) through the RAM domain (Furukawa et al., 1992; Schweisguth and Posakony, 1992; Tamura et al., 1995) and activates downstream target genes such as *HES1* and *HES5* (Jarriault et al., 1995; Kuroda et al., 1999; Ohtsuka et al., 1999). Four Notch receptors and its ligands are differentially and redundantly expressed in a variety of vertebrate tissues (Lardelli et al., 1994; Lardelli and Lendahl, 1993; Uyttendaele et al., 1996). On the other hand, the RBP-J protein is ubiquitously expressed (Hamaguchi et al., 1992) and commonly activated by all of four Notch receptors (Kato et al., 1996). Thus, RBP-J is an essential mediator of Notch signaling (Kato et al., 1997). In the absence of RAMIC, RBP-J represses transcription of target genes by associating with a corepressor complex containing SMRT (for silencing mediator for retinoid and thyroid hormone receptor) and a histone deacetylase (Kao et al., 1998). These corepressor proteins are dissociated from RBP-J upon interaction with RAMIC, which further recruits histone acetyltransferases PCAF and GCN5 to activate transcription (Kurooka and Honjo, 2000).

In *Drosophila* Notch signaling activity is negatively regulated by an intranuclear protein Hairless that interacts with Su(H) (Brou et al., 1994). Hairless is proposed to determine a threshold of Notch signaling activity (Bang et al., 1995). The generation of sensory organ precursors (SOP) from noncommitted precursors expressing both Notch and Delta is explained by the scenario that higher expression levels of Hairless in certain noncommitted precursors inhibit the differentiation suppression activity by Notch signaling and lead this population of progenitors to differentiation into SOP (Bang et al., 1995; Bang and Posakony, 1992). Thus, relative abundance of Hairless among noncommitted precursors that receive Notch signaling through mutual interaction can direct stable commitment to SOP. Neither a Hairless homolog nor other cell-specific regulatory molecules are known for vertebrate Notch. Since both

*Correspondence: honjo@mfour.med.kyoto-u.ac.jp
[4]These authors contributed equally to this work.

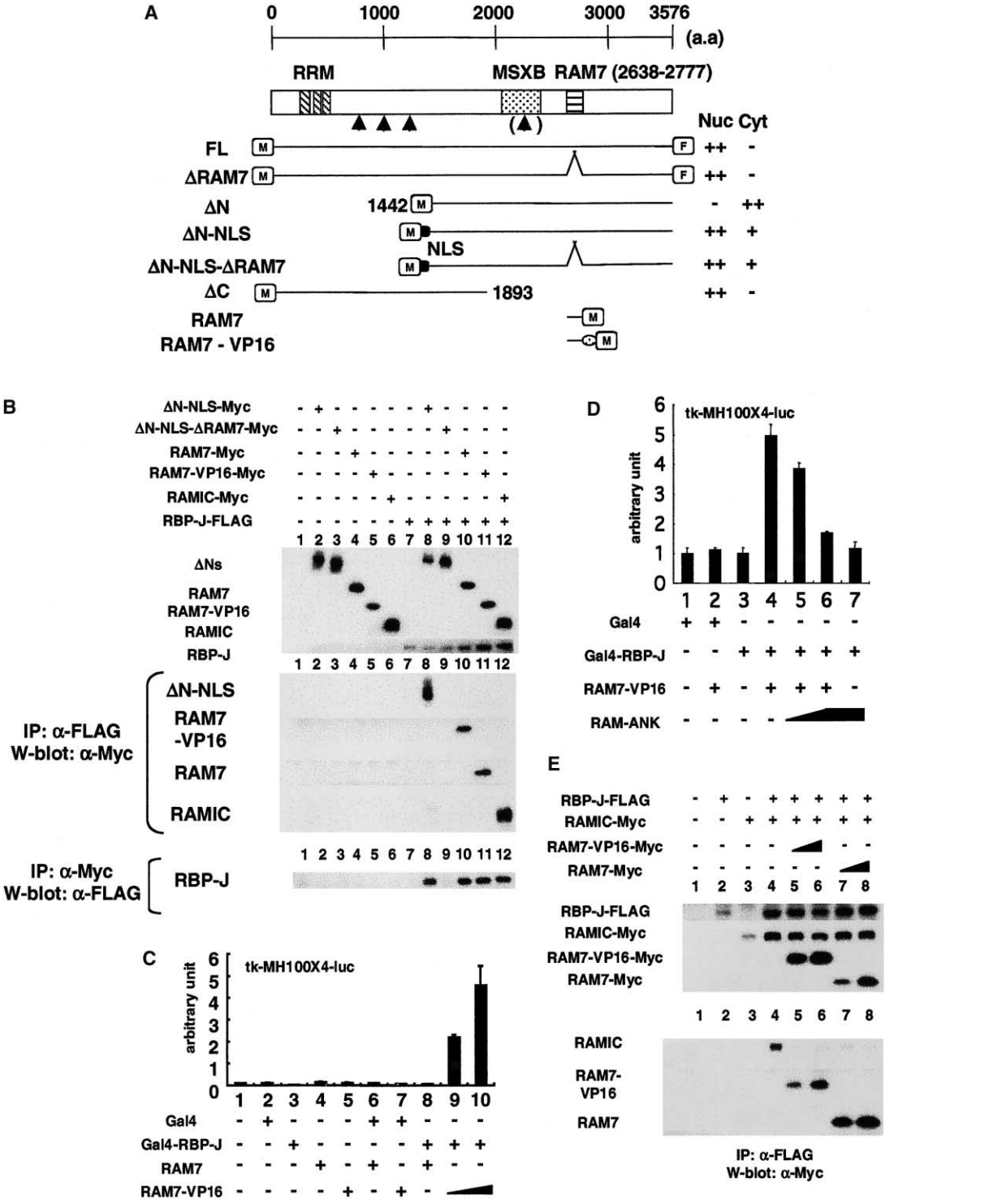

Figure 1. Functional and Physical Interaction of MINT with RBP-J

(A) Schematic representation of the mouse MINT (rectangle) and its derivatives (horizontal lines). Diagonal-hatched, dotted, and horizontal-hatched boxes indicate the RNA recognition motif (RRM), MSX2 binding domain (MSXB), and RBP-J binding domain (RAM7), respectively. The arrowheads, M boxes, and F boxes indicate the predicted nuclear localization signals (NLS), Myc-tag, and FLAG-tag, respectively. The NLS in MSXB was not functional because MINTΔN was not found in nuclei. The black ellipse and dotted circle indicate the SV40 NLS and VP16 activation domain, respectively. Intracellular localization of each construct in cultured cells is determined by immunofluorescence staining with anti-Myc or anti-FLAG antibody and shown at right. Nuc, nuclear; Cyt, cytoplasmic.

(B) Immunoprecipitation assays to detect the association of MINT and RBP-J. Two percent of the whole-cell extracts were analyzed by Western blotting with anti-Myc or anti-FLAG antibody (upper panel). Lysates from 293T cells transfected with plasmids indicated above were precipitated with the antibody indicated (IP), and the immunocomplexes were analyzed by Western blotting (W-blot) with the antibody indicated (lower two panels).

RBP-J and its interacting proteins are ubiquitously expressed, it is unknown how Notch/RBP-J signaling regulates differentiation from a common progenitor into two different lineages in vertebrates.

During yeast two-hybrid screening to identify RBP-J-interacting proteins (Tamura et al., 1995; Taniguchi et al., 1998) we isolated a cDNA fragment encoding mouse MINT (Msx2-interacting nuclear target protein) that has been previously reported to negatively regulate transcription by binding to a homeodomain transcriptional repressor protein MSX2, the murine homolog of *Drosophila* muscle-segment homeobox (Newberry et al., 1999) or to RAR (retinoic acid receptor) (Shi et al., 2001). We show here that the MINT protein, which is expressed in restricted tissues and cells, bound to a specific domain of RBP-J and repressed the RBP-J-mediated transcriptional activity by mouse Notch RAMIC. Since MINT-deficient mice were embryonic lethal, we studied differentiation of B lymphocytes in *RAG2*-deficient (therefore lymphocyte-deficient) mice, after transfer of *MINT*$^{-/-}$ fetal liver cells. *MINT*-deficient B cells differentiated preferentially into MZ B cells, thus providing the evidence that MINT negatively regulates Notch activity in a cell type-specific manner.

Results

Mouse MINT Binds to RBP-J

To search proteins that associate with the mouse RBP-J protein and regulate Notch signaling in nuclei, we performed yeast two-hybrid screening of cDNA libraries from mouse embryos (embryonic day 9.5) and HeLa cells using mouse RBP-J (RBP2) as a probe (Tamura et al., 1995; Taniguchi et al., 1998). Of 60 positive clones isolated, Notch1 (RAM23) (Tamura et al., 1995) and Kyo-T (RAM14) (Taniguchi et al., 1998) were previously reported. Among other positive clones we found a clone named RAM7 homologous to a portion (amino acids 2638–2777) of mouse MINT cDNA (Newberry et al., 1999) (Figure 1A).

The physical interaction of MINT with RBP-J was confirmed by the immunoprecipitation assay. Since the full-length (FL) MINT protein was too large to be solubilized from transfected cells, we used deletion constructs for the coimmunoprecipitation assay. Myc-tagged MINT fragments (ΔN-NLS, ΔN-NLS-ΔRAM7, RAM7, or RAM7-VP16) (Figure 1A) were expressed in 293T cells together with FLAG-tagged RBP-J, and their complex was immunoprecipitated using the anti-Myc or anti-FLAG monoclonal antibody and analyzed by Western blotting. The anti-Myc antibody coimmunoprecipitated RBP-J with MINT fragments containing the RAM7 domain (ΔN-NLS, RAM7, or RAM7-VP16) but not with ΔN-NLS-ΔRAM7 (Figure 1B, lower panel). Conversely, the anti-FLAG antibody coimmunoprecipitated only the RAM7-containing MINT fragments (ΔN-NLS, RAM7, or RAM7-VP16) with RBP-J (Figure 1B, middle panel). ΔN is not located in the nucleus and is unable to interact with RBP-J (data not shown). These results indicate that the MINT RAM7 domain is critical for its interaction with RBP-J.

To further confirm the interaction between the RAM7 domain of MINT and RBP-J in the nuclei, mammalian two-hybrid assays were performed using luciferase reporter constructs carrying the reiterated Gal4 binding sites. A fusion construct of mouse RBP-J with the Gal4 DNA binding domain (1–147) and another fusion construct of mouse RAM7 with the transactivation domain of VP16 (RAM7-VP16) (Figure 1A) were transiently cotransfected into NIH3T3 cells. The Gal4-dependent luciferase activity by the tk-MH100X4-luc reporter construct was augmented up to about 130 folds by increasing amounts of RAM7-VP16 (Figure 1C), suggesting a physical interaction of mouse RAM7 with RBP-J in nuclei.

We then examined whether RAM7 interferes in the binding of Notch RAMIC with RBP-J. Increasing amounts of the RAM-ANK fragment of RAMIC, which has only the RBP-J binding domain but not transactivation domain, gradually decreased the luciferase activity induced by interaction between Gal4-RBP-J and RAM7-VP16 (Figure 1D). Inversely, the luciferase activity induced by interaction between RAMIC and Gal4-RBP-J was reduced by increasing amounts of the RAM7 domain of MINT (data not shown). Furthermore, we confirmed that RAM7-VP16-Myc or RAM7-Myc competed with RAMIC-Myc for binding to RBP-J-FLAG (Figure 1E). These results taken together indicate that the RAM7 domain of MINT and the RAM domain of Notch compete with each other for physical interaction with RBP-J.

MINT Represses the RBP-J-Mediated Transcriptional Activity of Notch RAMIC

Since MINT was shown to compete for RBP-J binding with Notch, we examined the effect of MINT on Notch transactivation activities of promoters containing the RBP-J binding sites in NIH3T3 cells. Using the luciferase reporter construct carrying either the *HES1* or *Tp1* promoter that contains 2 and 12 tandem copies of RBP-J binding sites, respectively, we found that FL MINT

(C) Mammalian two-hybrid assays to detect the interaction between MINT (RAM7) and RBP-J. Five hundred nanograms each of pEF-BOS Neo/Gal4, pEF-BOS Neo/Gal4-RBP-J, pEF-BOS Neo SE/RAM7, and 250 or 500 ng RAM7-VP16 were cotransfected with tk-MH100X4-luc as a reporter plasmid into six wells each of NIH3T3 cells in an indicated mixture. Luciferase activity was measured as described in the Experimental Procedures.

(D) Competition between MINT (RAM7) and Notch1 RAMIC for binding to RBP-J was examined by mammalian two-hybrid assays. Ten nanograms of pCMX-Gal4, 10 ng of Gal4-RBP-J, 100 or 1000 ng of pEF-BOS Neo/RAM-ANK, and 50 ng of pEF-BOS Neo SE/RAM7-VP16 were cotransfected with tk-MH100X4-luc as a reporter plasmid into six wells of NIH3T3 cells in an indicated mixture.

(E) Competition between RAM7 and RAMIC for binding to RBP-J was examined by immunoprecipitation assays. One microgram of pEF-BOS Neo SE/RBP-J-FLAG, 1 μg of pEF-BOS Neo/Notch1 RAMIC, and 0.5 or 3 μg of pEF-BOS Neo SE/RAM7-VP16 or RAM7 were cotransfected into 6 cm dish of 293T cells. Two percent of the whole-cell extracts were analyzed by Western blotting with anti-Myc or anti-FLAG antibody (upper panel). Extracts of transfectants were immunoprecipitated by anti-FLAG, and precipitates were visualized using anti-Myc (lower panel).

(C–E) Triangles indicate increasing amounts of DNA. Means and standard deviations (SD) are calculated from three sets of experiments and are shown by bars and lines, respectively.

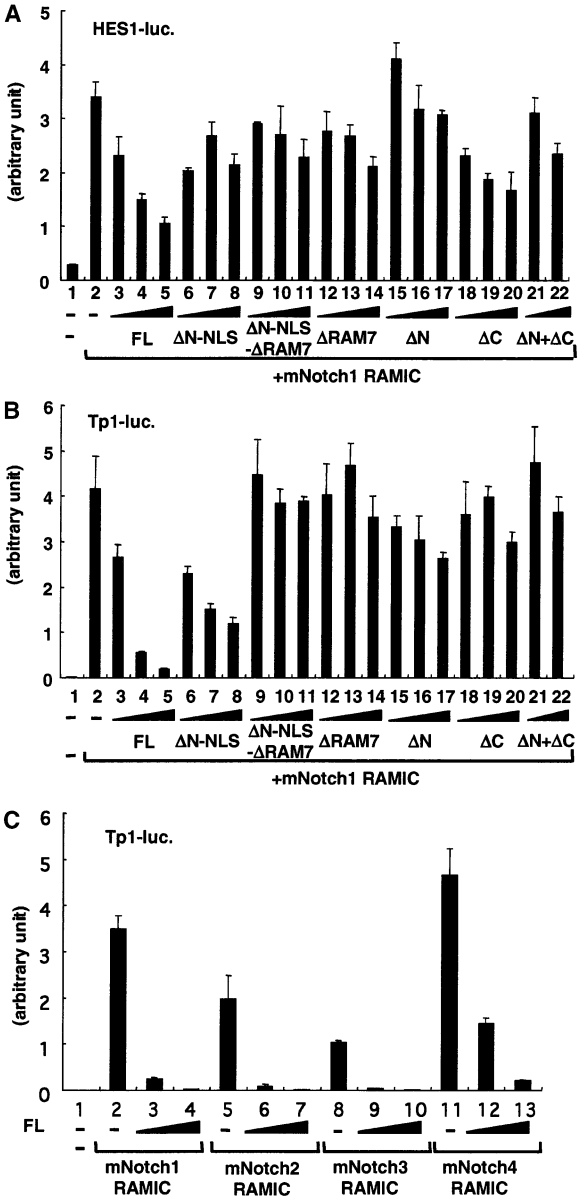

Figure 2. MINT Represses RBP-J-Mediated Transcriptional Activity

(A and B) Requirement of MINT FL for inhibition of Notch1 RAMIC-induced transcriptional activity.

(C) MINT FL repressed all four Notch RAMIC-induced transcriptional activity. Various amounts (either 30, 100, and 300 ng or 30 and 100 ng) of pEF-BOS Neo SE/MINT and its derivatives and 10 ng of pEF-BOS Neo/RAMIC were cotransfected into NIH3T3 cells (six wells) with p*HES1*-luc (A) or *Tp1*-luc (B and C) as a reporter plasmid. Excess amounts of MINT plasmids were added because of inefficient protein synthesis (see Supplemental Figure S2 at http://www.immunity.com/cgi/content/full/18/2/301/DC1). Mean values and SD are shown by bars and lines, respectively.

strongly inhibited RBP-J-mediated transcriptional activity of Notch in a dose-dependent manner (Figures 2A and 2B). MINT ΔRAM7 and MINT ΔC lacking the RAM7 domain had little, if any, repressive effects on transactivation by Notch, whereas the luciferase activity was slightly reduced by MINT ΔN-NLS. The difference in the suppressive activity between MINT ΔN-NLS and MINT FL suggests that the N-terminal region of MINT is required for the full repressive activity of MINT.

MINT was predicted to be cleaved by an unknown protease, resulting in accumulation of the N-terminal and C-terminal MINT fragments in chromatin and nuclear matrix fractions (Newberry et al., 1999). However, combination of the N-terminal and C-terminal fragments of MINT cannot exert a stronger suppressive activity than each of them, indicating that full repression of RBP-J-mediated transcription requires the intact MINT FL molecule (Figures 2A and 2B).

To examine whether MINT represses RBP-J-mediated transcriptional activity by the other Notch members, MINT FL and Notch2-4 RAMIC plasmids were cotransfected with the *Tp1*-luc reporter into NIH3T3 cells (Figure 2C). MINT strongly repressed the RBP-J-mediated transcriptional activity by all four Notch family members (Figure 2C), indicating that MINT is a common suppressor of RBP-J-mediated transcriptional activity of all Notches.

Targeted Disruption of the *MINT* Gene

Although RBP-J is ubiquitously expressed, *MINT* transcripts were found in limited tissues including testis, brain, spleen, lung, liver, and kidney (Newberry et al., 1999). Little expression of *MINT* mRNA was detected in cardiac and skeletal muscle, or ovary. These results suggest that *MINT* might be involved in tissue-specific regulation of Notch signaling. To test this possibility, we generated *MINT* gene knockout mice by homologous recombination in ES cells. To introduce a targeted mutation in the mouse *MINT* gene, we constructed a targeting vector, in which the expression cassette of the *neomycin resistance* (*neo*) gene was inserted in the 5′ region of an exon encoding the MSXB domain and flanked by the 5′ 6.6 kb and 3′ 3.4 kb *MINT* gene fragments (SpeI-XhoI) (Figure 3A). A *diphtheria toxin A* (*DT-A*) gene was placed outside the homologous region for negative selection.

The targeting vector was electroporated into mouse embryonic stem (ES) cells, and DNA isolated from G418-resistant ES clones was analyzed by Southern blotting analysis using probe A. The wild-type and disrupted alleles generated the 10.0 and 6.6 kb SpeI-XhoI fragments, respectively (Figure 3B). Of 124 ES cell clones screened, 72 contained the mutant allele and had undergone a homologous integration at the *MINT* locus. Two chimeric mice were generated from two independent ES cell clones, and germline transmission of the disrupted *MINT* allele was achieved from both of them. One line was backcrossed to C57BL/6J mice for seven to ten generations. Heterozygous mice were bred to produce homozygous mutant offsprings, and DNAs of these mice were analyzed by Southern blotting (Figures 3B) and PCR (data not shown).

No homozygous mutant pups with the *MINT* mutation ($MINT^{-/-}$) were born, indicating that disruption of the *MINT* gene is embryonic lethal. Northern blotting analysis showed that E12.5 $MINT^{-/-}$ homozygotes expressed truncated MINT mRNA as expected from insertion of the neo cassette (data not shown). $MINT^{-/-}$ homozygotes were found according to Mendelian segregation

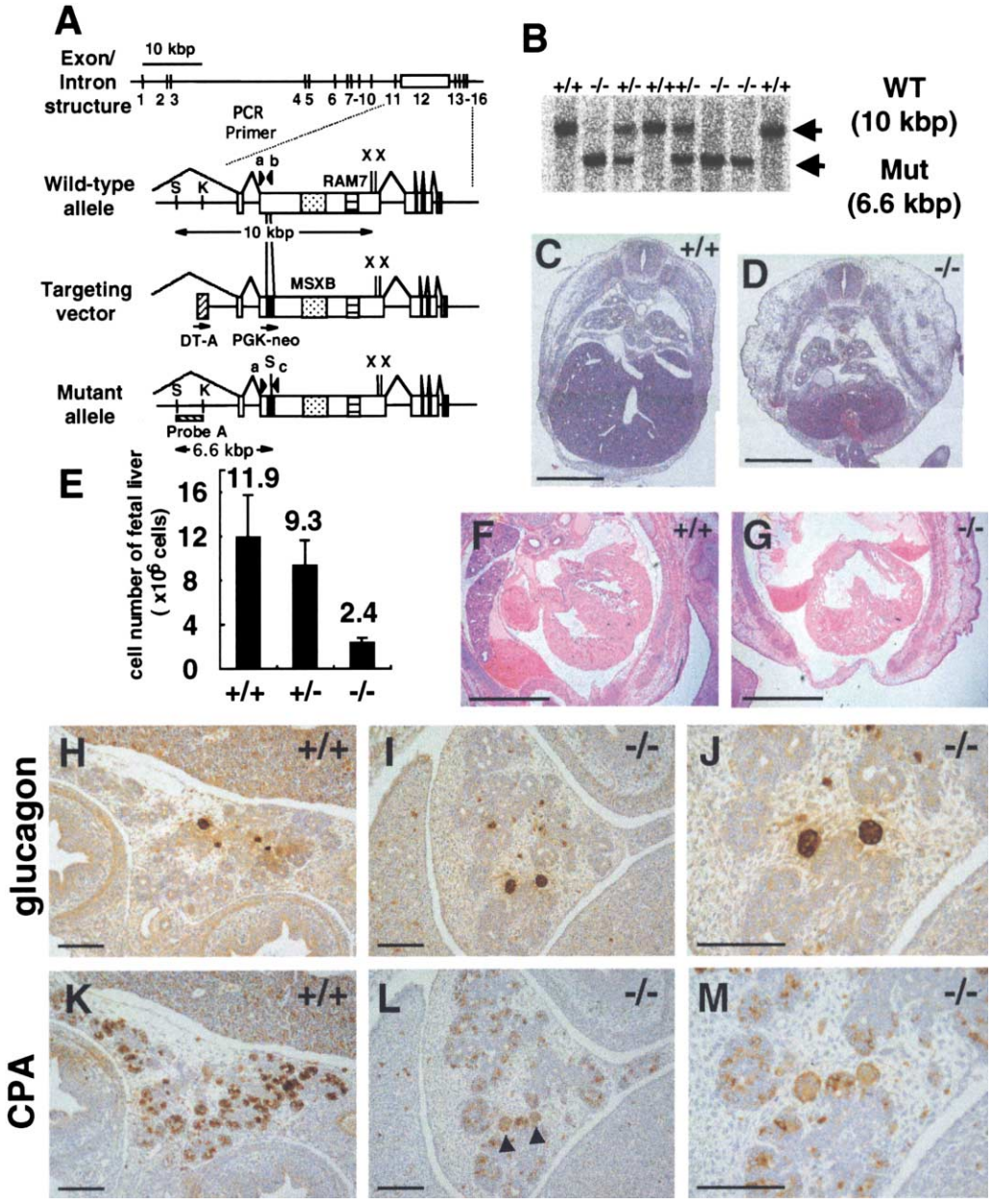

Figure 3. Generation of a Null Allele at the *MINT* Locus and Analysis of *MINT* Mutant Embryos

(A) Schematic representation of the wild-type *MINT* allele, the targeting vector, and the disrupted *MINT* allele generated by homologous recombination. K, KpnI; S, SpeI; X, XhoI; DT-A, diphthria toxin A. PGK-neo PCR primer used in (C) is indicated.

(B) Southern blot analysis of embryo DNA using probe A shown in (A). The 10 and 6.6 kb SpeI-XhoI fragments derived from the wild-type (WT) and the mutant (Mut) allele, respectively, are indicated.

(C, D, F, and G) Morphology of E13.5 $MINT^{+/+}$ (C and F) and $MINT^{-/-}$ embryos (D and G) at E13.5. Hematoxylin-eosin stained axial sections were shown.

(E) Reduction of fetal liver cell number in $MINT^{-/-}$ embryos. Five embryos of each genotype were sacrificed, and total fetal liver cells were counted after making single-cell suspension. Mean cell numbers and SD are shown by bars and lines, respectively.

(H–M) Immunohistochmistry performed on wild-type (H and K) and $MINT^{-/-}$ (I–J and L–M) embryonic pancreases with anti-glucagon (H–J) and anti-CPA (K–M) antibodies. (J and M) High-power view of the glucagon and CPA-double-positive cells (arrowheads in [L]) in $MINT^{-/-}$ pancreas. Bars, 1 mm in (C)–(G) and 0.1 mm in (H)–(M).

in embryos at E10.5 to E11.5 but were sharply reduced from E12.5, suggesting that embryonic lethality may start around E12 (Table 1). At E10.5, $MINT^{-/-}$ embryos appeared similar in size and morphology to the heterozygous ($MINT^{+/-}$) and wild-type ($MINT^{+/+}$) littermates. But by E13.5, $MINT^{-/-}$ embryos were severely affected as compared to wild-type embryos. The skin of $MINT^{-/-}$ embryos was loose and transparent with a large amount

Table 1. Genotype Frequency of Progenies from Intercrosses of MINT Heterozygous Mice

Stages	+/+ (%)	+/− (%)	−/− (%)
E10.5 (n = 7)	2 (29.6)	2 (29.6)	3 (40.8)
E11.5 (n = 9)	2 (22.2)	4 (44.4)	3 (33.4)
E12.5 (n = 33)	15 (45.4)	16 (48.5)	2 (6.1)
E13.5 (n = 102)	37 (36.3)	62 (60.8)	3 (2.9)
E14.5 (n = 62)	20 (32.3)	39 (62.9)	3 (4.8)
E16.5 (n = 15)	8 (53.3)	7 (46.7)	0 (0)

The numbers indicate embryos of each genotype. Total numbers of embryos for each gestation stage are shown by n. Percentages of each genotype are shown in parentheses.

of subcutaneous exudates, and their fetal liver was extremely smaller than in wild-type embryos (Figures 3C and 3D). Consequently, the total cell number in fetal livers of *MINT*$^{-/-}$ embryos fell below one-fourth of that in wild-type embryos (Figure 3E).

MINT$^{-/-}$ embryos displayed defect in formation of the cardiac septum and muscle (Figures 3F and 3G) in general agreement with the previous finding that Notch regulates heart development (McCright et al., 2001). Similarly, *MINT*$^{-/-}$ embryos were defective in differentiation of pancreatic cells, which was also reported in mice deficient for Delta1 or RBP-J (Apelqvist et al., 1999). Although cells expressing glucagon (endocrine cell marker) and carboxypeptidase A (exocrine cell maker, CPA) were formed in *MINT*$^{-/-}$ embryos, CPA expression was lower in *MINT*$^{-/-}$ pancreas, and some of the glucagon-positive cells of *MINT*$^{-/-}$ embryos also expressed CPA (Figures 3H–3M), suggesting that differentiation into exocrine and endocrine cells may be disturbed by MINT deficiency. These results support the idea that MINT is involved in regulation of Notch signaling.

Differentiation of *MINT*$^{-/-}$ Fetal Liver Cells

To investigate whether MINT regulates maturation of fetal liver cells, we investigated the number of erythroid- and myeloid-committed progenitors in the fetal liver cells using an in vitro colony-forming assay. The frequencies of BFU-E, CFU-E, and CFU-GM colonies from the fetal liver cells of *MINT*$^{-/-}$ embryos (E12.5) were indistinguishable from those of the control *MINT*$^{+/+}$ fetal liver cells (data not shown). Fluorescence activated cell sorter (FACS) analyses of these fetal liver cells did not reveal difference in the relative frequency of c-kit^{+}, CD45.2^{+}, and TER119^{+} cells between *MINT*$^{-/-}$, *MINT*$^{+/-}$, and *MINT*$^{+/+}$ littermates (data not shown).

To examine whether the differentiation of fetal liver cells into mature lymphocytes is affected by MINT deficiency, fetal liver cells from E12.5 *MINT*$^{-/-}$ embryos were transplanted into sublethally irradiated *RAG2*$^{-/-}$ mice that cannot generate any T and B lymphocytes (Shinkai et al., 1992). Although the total numbers of T and B cells in spleen were significantly reduced, their relative numbers in spleen, lymph nodes, and bone marrow were similar among *RAG2*$^{-/-}$ recipients of fetal liver cells from *MINT*$^{-/-}$, *MINT*$^{+/-}$ and *MINT*$^{+/+}$ embryos after 10–12 weeks of injection (Figure 4 and data not shown). Also, no differences in B-1 and B-2 B cell numbers in the peritoneal cavity was observed between *MINT*$^{-/-}$ cell and *MINT*$^{+/+}$ cell recipients (Figure 4D).

Splenic B cells are categorized according to their surface markers into transitional B cells, which are newly arrived from bone marrow (T1 and T2 B cells) and differentiated B cells (Fo and MZ B cells) (Loder et al., 1999; Oliver et al., 1997). The population of CD21^{hi} CD23^{lo} B220^{+} splenic cells that have been shown to be MZ B cells (Oliver et al., 1997) increased by more than 3-fold in the recipients of *MINT*$^{-/-}$ cells as compared with those of *MINT*$^{+/+}$ and *MINT*$^{+/-}$ cells (Figures 4A and 4E). The absolute numbers of MZ B cells also increased in *MINT*$^{-/-}$ recipients as compared with control recipients (Figure 4F).

To confirm the increase of the MZ B cells in *MINT*$^{-/-}$ fetal liver cell recipients, spleen cryosections were stained with anti-IgM and anti-MAdCAM-1 antibodies and examined by confocal microscopy (Figures 5A–5D). IgM^{lo} Fo B cells are surrounded by the MAdCAM-1 positive macrophages while IgM^{hi} MZ B cells are located outside the MAdCAM-1 positive layer. The width of MZ B cells, located outside of the MAdCAM-1 layer, thickened by about 2.5-fold in *MINT*$^{-/-}$ recipients (Figure 5E) and the ratio of MZ to Fo area increased by 1.7-fold in *MINT*$^{-/-}$ recipients (Figure 5F). These results suggest that MINT may be involved in differentiation of transitional B cells into MZ versus Fo B cells in spleen.

Since MZ B cells have been proposed to play a critical role in humoral responses, we analyzed basal serum amounts of IgM, IgG1, IgG2a, IgG2b, IgG3, and IgA. But we did not find significant differences except that the IgG2b concentration was slightly reduced in recipients of *MINT*$^{-/-}$ cells as opposed to those of *MINT*$^{+/+}$ or *MINT*$^{+/-}$ cells ($p < 0.01$) (data not shown). Little difference of the serum immunoglobulin isotype levels in mice with increased MZ B cells is consistent with the phenotype in MZ B cell null mice that is caused by B cell-specific RBP-J deficiency (Tanigaki et al., 2002).

MINT Expression and Subsets of Splenic B Cells

To identify the localization of MINT in spleen, we performed in situ hybridization analysis for MINT mRNA expression in serial sections of spleen (Figures 5G–5L) and found MINT mRNA expression in lymphoid follicles (Figures 5H and 5I). To examine the exact location and cell type of MINT expression in spleen, the image of MINT mRNA expression detected by in situ hybridization was overlaid with the immunostaining on the serial spleen sections using anti-MAdCAM1 and anti-IgM (Figure 5K) antibodies which dominantly stain metallophilic macrophages and MZ B cells, respectively. The double images clearly indicated that MINT mRNA expression was strong in the Fo B cell zone but less in the MZ B cell zone (Figure 5L). Since in situ hybridization is not quantitative at all, Southern blotting analysis of RT-PCR products was performed on the sorted B cell populations. In general accordance with in situ data, MINT mRNA expression was two to three times higher in Fo B cells than in T1, T2, and MZ B cells (Figure 6A). Expression of Notch2 was strongest in Fo B cells, followed by T1 cells. Spleen cell types other than B cells had very weak Notch2 expression (Figure 6B). Notch1, 3, and 4 mRNAs were not expressed or were weakly expressed in splenic B cells (data not shown). Conversely, the expression of HES1 mRNA, one of the Notch/RBP-J signal-

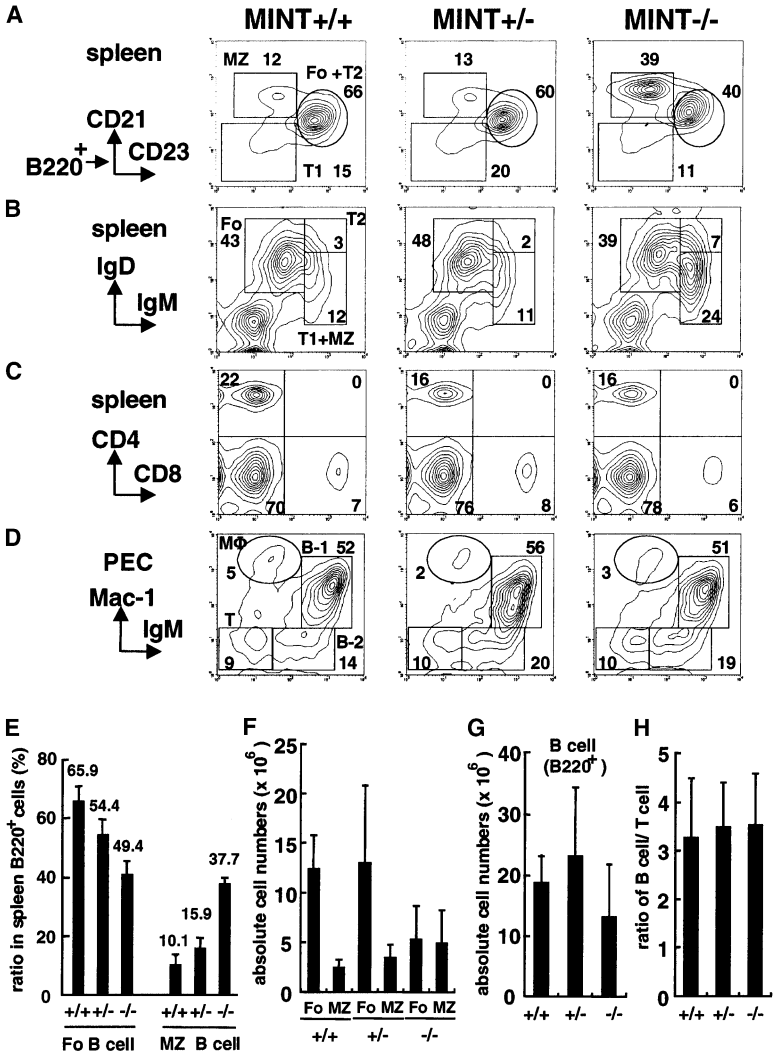

Figure 4. Increase in MZ B Cell Differentiation from *MINT*-Deficient Fetal Liver Cells

(A) 8 × 10^5 fetal liver cells from *MINT*$^{+/+}$, *MINT*$^{+/-}$, and *MINT*$^{-/-}$ at E12.5 embryos were transferred i.v. into lethally irradiated *RAG2*$^{-/-}$ mice. After 10 weeks, FACS analyses of erythrocyte-depleted splenocytes (A–C) and peritoneal cavity cells (D) were performed to determine the cell surface expression of CD21 and CD23 of B220$^+$ sated cells for (A), IgM and IgD for (B), CD4 and CD8 for (C), and Mac-1 and IgM for (D). Panels are representative of at least two analyses using at least three mice for each genotype. (E) The percentages of Fo and MZ B cells were estimated by FACS staining shown in (A). The absolute numbers of Fo and MZ B cells (F) and B cells (G) in spleen were estimated by FACS staining. (H) The ratio of B to T cell number in spleen is shown. Bars show mean ±SD obtained from three mice. T1, transitional B cell of type 1; T2, transitional B cell of type 2; Fo, follicular B cell; MZ, marginal zone B cell; T, T cell; Mϕ, macrophage; PEC, peritoneal cavity.

ing targeted genes, was much decreased in Fo B cells as compared with the other splenic B cells probably because of inhibition of Notch signaling by higher concentrations of MINT (Figure 6A). Expression levels of Cμ, CD21, and CD23 were in good agreement with FACS profiles of each subpopulation of splenic B cells.

Notch ligands were reported to be expressed in splenic macrophages and dendritic cells (DCs) (Yamaguchi et al., 2002). To confirm the expression of Notch ligands in spleen, we performed RT-PCR analysis. Expression of Delta3, Jagged1, and Jagged2 mRNAs was not detected in spleen (Figure 6B). Delta1 and 4 expression was detected in whole spleen but not erythrocyte-depleted splenocytes, B (B220$^+$) cells, and T (CD4$^+$ or CD8$^+$) cells. This suggested that other cells, probably DCs, which are lost during erythrocyte depletion, might express Notch ligands. Indeed, CD11c$^+$ DCs expressed Delta1 and Delta4 mRNAs. Because DCs are distributed in splenic MZ as well as T cell zone (Steinman et al., 1997), it is likely that Notch ligands expressed on DCs might be affecting the commitment of Notch-MINT-expressing T1 B cells into either MZ or Fo B cells.

To examine the localization of Notch2-expressing cells in spleen, histological analysis was performed by using *Notch2-lacZ* mice (Hamada et al., 1999). The lacZ-positive cells were found scattered in the follicle and lined along MZ (Figure 6D) by β-Gal staining. To further confirm the exact location of lacZ-positive cells in spleen, the image of Notch2 expression was overlaid with the immunostaining on the serial spleen section using anti-MAdCAM1. The double images clearly indicated that Notch2-expressing cells were lined immediately outside the MAdCAM1-expressing metallophilic macrophage in the marginal sinus (Figures 6C–6E). Since Notch2 is most strongly expressed on Fo and T1 B cells (Figures 6A and 6B), Notch2-expressing cells in MZ are likely to be T1 B cells. These results suggest that Notch2-expressing T1 B cells may interact with DCs in MZ and differentiate into either MZ or Fo B cells depending on the relative abundance of MINT.

Discussion

We have identified a negative regulator of Notch signaling by yeast two-hybrid screening using RBP-J as a bait. This molecule, previously identified as MINT, competed

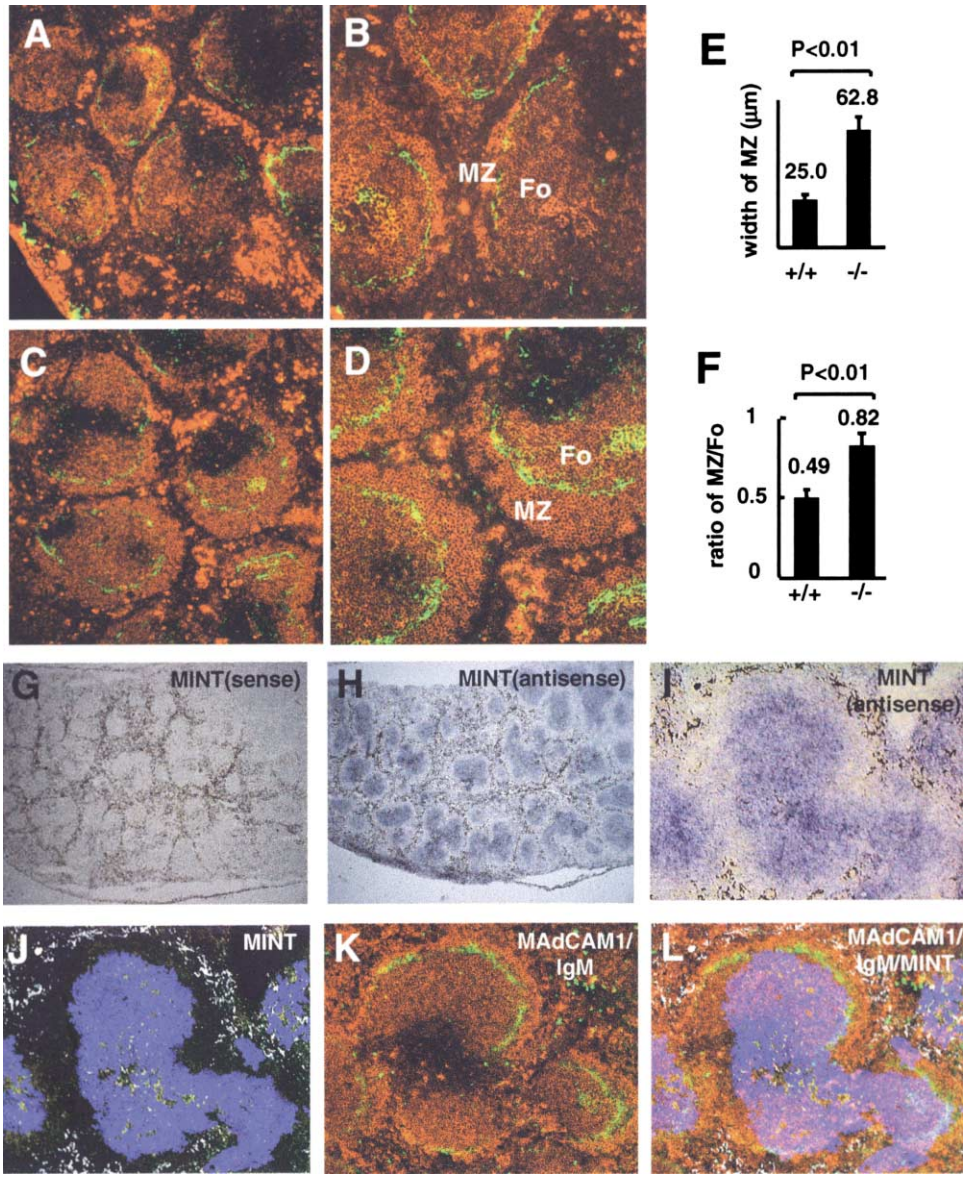

Figure 5. Immunohistochemical Analysis of *MINT*$^{-/-}$ Fetal Liver Transferred *RAG2*$^{-/-}$ Spleen

(A–D) Serial sections of spleen were prepared from recipients of *MINT*$^{+/+}$ (A and B) and *MINT*$^{-/-}$ (C and D) fetal liver. Immunofluorescence microscopic study was performed to detect MZ and Fo zone with anti-MAdCAM-1 (green) and anti-IgM (red) antibodies. The two images were superimposed (A–D). (B and D) High-power view of (A) and (C), respectively, at the same magnification. The width of MZ (E) and the ratio of MZ area to Fo area (F) were calculated from images of immunohistochemistry slides. Bars show mean ±SD obtained from measurements of total 11 points of five follicles (E) and five follicles (F) in each genotype. (G–L) Localization of *MINT* mRNA by in situ hybridization in spleen. (G) *MINT* sense probe, (H and I) *MINT* antisense probe, and (J) electronically converted image of (I) into blue. (K) anti-IgM (red) and anti-MAdCAM1 (green). (L) Superimposed images indicated.

with Notch RAMIC for binding to RBP-J and repressed the RBP-J-mediated transactivation activity by mNotch1-4 RAMIC as measured by the *HES-1* and *Tp1* promoter assay. To confirm negative regulation of Notch signaling by MINT in vivo, we have generated MINT-deficient mice, which died around day 14.5 with morphological abnormality in pancreas and heart. Embryogenesis of these organs is known to be regulated by Notch (Apelqvist et al., 1999; McCright et al., 2001). Since deficiency of RBP-J (Tanigaki et al., 2002) and Notch2 (H. Hirai, personal communication) almost completely abolishes MZ B cells and increases Fo B cells, activation of Notch signaling is expected to enhance MZ B cell differentiation and to block Fo B cell differentiation. Indeed, splenic B cells derived from MINT-deficient fetal liver cells were facilitated to differentiate into MZ B cells while differentiation into Fo B cells was suppressed. It is therefore likely that higher expression levels of MINT in progenitor B cells block their differentiation into MZ B cells by suppressing Notch signaling and allow them to become Fo B cells. Recently, negative regulation of Notch signaling by SHARP (the human homolog of MINT) was also

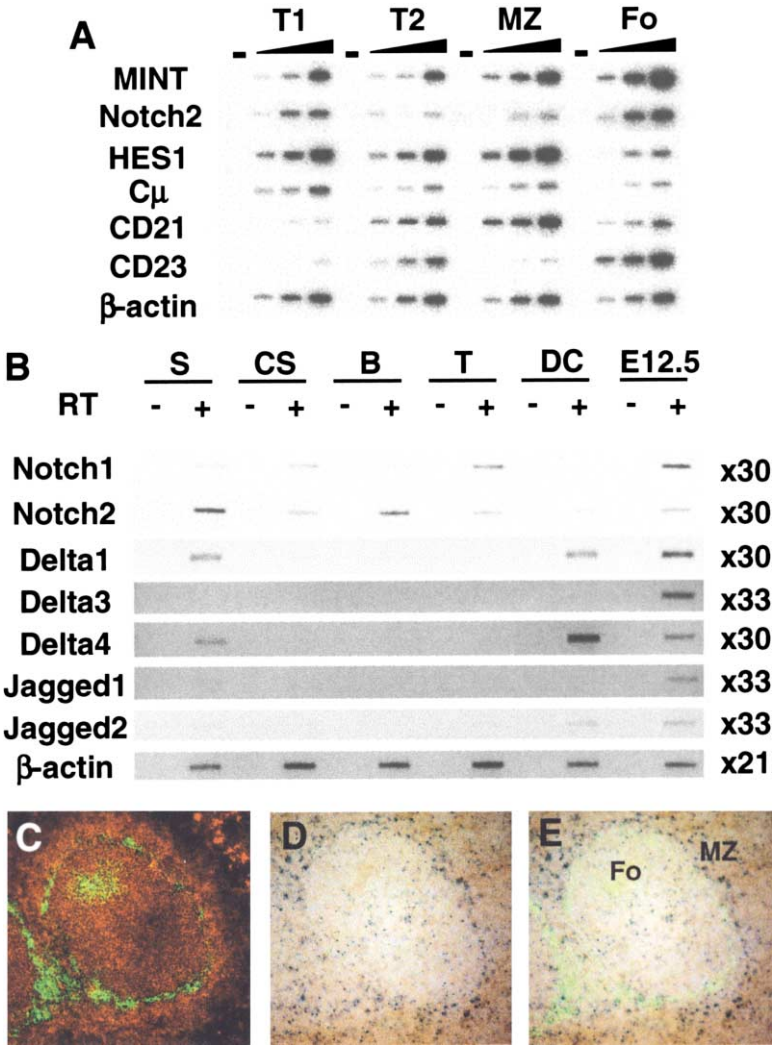

Figure 6. RT-PCR Analysis of MINT and Markers in T1, T2, MZ, and Fo B Cells

(A) Three-hold serial dilutions of cDNA transcribed from RNA isolated from 2×10^5 cells of sorted population of B cells were amplified with specific primers, blotted, and hybridized with an appropriate probe.

(B) RT-PCR analysis of Notch receptors and ligands expression in spleen. Numbers of PCR cycles are indicated at right. RT, reverse transcriptase; S, total spleen; CS, cell suspension of erythrocyte-depleted splenocytes; B, $B220^+$ B cells; T, $CD4^+$ or $CD8^+$ T cells; DC, $CD11c^+$ dendritic cells; E12.5, whole embryos at day 12.5.

(C–E) Localization of Notch2-expressing cells by using *Notch2-lacZ* mouse spleen and β-Gal staining. (C) anti-IgM (red) and anti-MAdCAM-1 (green), (D) β-Gal staining of Notch2 expression (blue), and (E) β-Gal staining of Notch2 expression and anti-MAdCAM-1 (green).

demonstrated in neurogenesis of *Xenopus* embryos (Oswald et al., 2002).

Stronger expression of Notch2 on T1 B cells and Notch ligands (Delta1 and Delta4) on DCs suggests that Notch signaling may be activated upon interaction between Notch2-expressing T1 B cells and Delta1 and/or 4-expressing DCs at the marginal sinus. Since Notch signaling is not required for Fo B cell differentiation, not all Fo B cells had interacted with DCs. Indeed, MINT expression was only a few times higher in Fo B cells than in MZ B cells, yet HES1 expression was severely reduced in Fo B cells. We propose that T1 B cells which have not met DCs and thus not received Notch signaling will differentiate into Fo B cells. Among those that have interacted with DCs, the $MINT^{hi}$ cells differentiate into Fo B cells by inhibiting Notch signaling activity, while $MINT^{lo}$ cells differentiate into MZ B cells by strong Notch signaling activity. Thus, MINT regulates negatively Notch signaling and determines the subset commitment of splenic B cells. No changes in the pro-B cells fraction were found in bone marrow (see Supplemental Figure S1 at http://www.immunity.com/cgi/content/full/18/2/301/DC1). Since the ratio of T and B cells was not affected in recipients of $MINT^{-/-}$ fetal liver cells, not all Notch pathways appear to be regulated by MINT.

The biased expression of the negative regulator of Notch signaling, MINT in the binary cell fate decision system is reminiscent of the hypothesis to explain *Drosophila* SOP commitment by expression levels of Hairless in noncommitted precursors expressing both Notch and Delta (Bang et al., 1995). In this hypothesis noncommitted precursors with higher levels of Hairless inhibit Notch signaling activated by interaction with neighboring precursors, resulting in commitment to SOP, while those with lower levels of Hairless remain noncommitted precursors by strong Notch signaling (Bang and Posakony, 1992). Hairless competes with Notch for binding to the *Drosophila* ortholog of RBP-J, i.e., Su(H), and suppresses transcription by recruiting the *Drosophila* C-terminal binding protein (dCtBP) which acts as a transcriptional corepressor (Morel et al., 2001).

RBP-J has been reported to interact with a histone deacetylase (HDAC) corepressor complex including SMRT, Sin3A (mammalian ortholog of the yeast SIN3 corepressor), CIR (C promoter binding factor 1 interacting corepressor), and HDACs, which causes repres-

sion of Notch target genes in the absence of RAMIC (Hsieh et al., 1999; Kao et al., 1998). These corepressor proteins are dissociated from RBP-J upon interaction with RAMIC that recruits histone acetyltransferase PCAF and GCN5 (Kurooka and Honjo, 2000), resulting in activation of Notch target gene transcription. One of possible MINT functions could therefore be recruitment of the HDAC corepressor complex. Interestingly, transfected MINT proteins were detected as speckles in nuclei as reported for SMRT (Zhou and Hayward, 2001) and HDAC (Hsieh et al., 1999), and the human MINT ortholog, SHARP, was shown to bind to the SMRT and HDAC1 (Shi et al., 2001). However, the transcriptional repression by MINT in Notch signaling was not blocked by trichostatin A, an inhibitor of the HDAC activity (data not shown), suggesting that the HDAC complex may not be involved in the suppressive activity of MINT. In fact, the human MINT ortholog, SHARP, was shown to inhibit the RAR-mediated transactivation by binding to RAR and the steroid receptor RNA coactivator SRA (steroid receptor RNA activator), thus preventing their direct interaction (Shi et al., 2001).

MINT is found to inhibit expression of the osteocalcin gene through the interaction with the MSX2 protein (Newberry et al., 1999). In addition, *split ends* (*spen*) (Kuang et al., 2000; Wiellette et al., 1999), the *Drosophila* homolog of MINT, is shown to be a transcriptional repressor involved in function of *yan*, one of the target genes of the RTK/Ras/MAPK pathway (Rebay et al., 2000). Therefore, MINT may be involved in transcriptional repression in various systems other than Notch.

In summary, we have shown that MINT suppresses generation of MZ B cells probably through negative regulation of Notch activity. Cell-specific expression of MINT can explain the mechanism for binary cell fate decision by Notch in mammalian systems, suggesting that MINT may be a mammalian functional homolog of *Drosophila* Hairless.

Experimental Procedures

Cloning of MINT cDNA and Construction of Its Derivatives

A HeLa cell cDNA library was screened by the yeast two-hybrid method with mouse RBP-J as a bait (Tamura et al., 1995; Taniguchi et al., 1998). The resulting human RAM7 cDNA was used as a probe to screen the cDNA library from mouse 9.5 dpc embryos (Clontech). Myc-MINT (FL, amino acids 1–3576)-Flag, Myc-MINTΔRAM7 (2638–2777)-FLAG, Myc-MINTΔN (1442–3576), Myc-SV40 NLS-MINTΔN (1442–3576), Myc-SV40 NLS-MINTΔN-ΔRAM7 (Δ2638–02777), Myc-MINTΔC (1–1893), Myc RAM7 (2638–2777), and Myc-RAM7-VP16 were ligated into pEF-BOS Neo SE vector derived from pEF-BOS Neo (Kuroda et al., 1999; Mizushima and Nagata, 1990). pEF-BOS Neo/Notch1-4 RAMIC, pEF-BOS Neo/Notch1 RAM-ANK, pEF-BOS Neo SE/ RBP-J-FLAG, tk-MH100X4-luc, p*HES1*(1.0 kb)-luc, pGa981-6 (*Tp1*-luc), and pCMX-lacZ or pRL-CMV (Promega) were previously described (Kurooka et al., 1998; Minoguchi et al., 1997; Mizutani et al., 2001; Takebayashi et al., 1994). All Notch and RBP-J used are derived from mouse.

Luciferase Assay

NIH3T3 cells seeded in 6-well plates (35 mm) were transfected with the plasmids indicated and 200 ng pCMX-lacZ or 50 ng pRL-CMV (Promega) using Lipofectamine (Invitrogene). Transfected cells were harvested around 24 hr after transfection, and luciferase activities in the cell extracts were measured according to the manufacturer's instructions (Promega) in a luminometer (Microplate luminometer LB96V, Berthold). Luciferase activities as indicated by arbitrary unit were normalized by β-Gal or sea urchin luciferase activities in each sample. All experiments were repeated at least three times, and the averages of more than three independent experiments with standard deviations are shown as bars.

Immunoprecipitation Analysis

Immunoprecipitation was done as described previously (Minoguchi et al., 1997) with either the anti-Myc (9E10) (Santa-Cruz) or anti-FLAG M2 (Sigma) monoclonal antibodies.

Immunohistochemical Examination

Tissue sections (12 μm) of spleen were prepared, fixed in 4% paraformaldehyde/PBS (−) for 10 min, blocked with 25% goat serum/PBS (−) for 10 min, and stained with anti-MAdCAM-1 (clone MECA-367; PharMingen), anti-mouse IgD (clone SBA1; Southern Biotechnology), anti-IgM-rhodamine (Cappel), and anti-rat IgG-FITC (Jackson Laboratory). Slides were mounted in SlowFade Light antifade Kit Component A (Molecular Probes) and analyzed with a Bio-Rad confocal laser scanning microscope (model MRC-1024). The spleen of *Notch2-lacZ* mice was fixed with 2% paraformaldehyde, 0.2% glutaraldehyde, PBS (−) and stained with X-gal. For histological study of embryonic pancreas, whole embryos were fixed with Bouin's solution, embedded in paraffin, and cut at 3.5 μm thickness. After deparaffinization, endogenous peroxidase was inhibited with 0.3% hydrogen peroxide in methanol for 20 min, and blocked with normal goat serum (Dako). Rabbit antibody anti-glucagon (Linco) or carboxypeptidase A (Chemicon), biotin-labeled goat anti-rabbit IgG serum, and avidin-biotin complex were sequentially used. Substrate for peroxidase (3,3′-diaminobeizidine) was obtained from Dako.

In Situ Hybridization

Cryosections (8–12 μm) from normal spleen were fixed in 4% paraformaldehyde. In situ hybridization was performed as described previously (Braissant et al., 1996). The antisense probe was transcribed from the 1958 bp EcoRI-BamHI fragment (nucleotides 1150–3107) of MINT.

Generation and Genotyping of *MINT* Mutant Mice

Homologous recombination was used to disrupt the *MINT* gene in ES cells. *MINT* genomic fragments were cloned by screening of a phage library containing 129/Sv mouse DNA fragment. To construct the targeting vector, a neomycin phosphotransferase-expressing cassette (PGK-neo) was inserted between the SmaI (nucleotide 4510 of the coding region) and HindIII (nucleotide 4891 of the coding region) sites to replace the region between the two restriction sites. A dyphtheria toxin A (DTA)-expressing cassette was flanked outside the 3′ homologous region. The vector was linearized by restriction digestion and used to transfect ES cell line E14 by electroporation. Transfected cells were cultured in the presence of G418 (300 μg/ml), and G418-resistant clones were expanded and screened by Southern blotting analysis using a fragment outside the 5′ homologous region as a probe (probe S-K). ES clones with homologous recombination were microinjected to blastocysts from C57BL/6 mice to generate chimeras. Chimeras were bred with C57BL/6 to get germline transmission of the mutant *MINT* allele.

Reconstitution of the Lymphoid Compartment in *RAG2*$^{-/-}$ Mice

Fetal liver cells (1×10^6) from E12.5 *MINT*$^{+/+}$, *MINT*$^{+/-}$, and *MINT*$^{-/-}$ embryos were injected intravenously into 4 Gy irradiated *RAG2*$^{-/-}$ mice (Shinkai et al., 1992). After 10–12 weeks, single-cell suspensions were prepared from spleens and peritoneal cavities of the reconstituted *RAG2*$^{-/-}$ mice and subjected to FACS and immunohistochemical analyses. The following monoclonal antibodies were used: fluorescein isothiocyanate (FITC)-conjugated anti-CD21 (7G6), phycoerythrin (PE)-conjugated anti-CD23 (B3B4) and anti-CD4 (GK1.5), and allphycocyanin (APC)-conjugated anti-B220 (RA3-6B2), anti-CD8 (53-6.7) and anti-Mac1/CD11b (M1/70) (PharMingen). The following polyclonal antibodies were used: FITC-conjugated anti-IgM and PE-conjugated anti-IgD (Southern Biotechnology). All FACS analyses were performed on a FACSCalibur (Becton-Dickinson). Data were obtained by analysis of $1–2 \times 10^4$ viable cells, as determined by forward light-scatter intensity and propidium iodide gating.

RT-PCR Analysis of Gene Expression

Total RNAs were prepared from 2×10^5 each of sorted B cell populations (expressing appropriate phenotypes) by TRIzol (GIBCO). cDNA synthesis and PCR were done as previously described (Minoguchi et al., 1997). The PCR products were separated on an agarose gel, blotted, and hybridized with an appropriate cDNA fragment. As a control, PCR products with β-actin primers were analyzed by BAS system (Fuji film).

DCs were prepared from spleen by collagenase digestion, as previously described for gut lamina propria lymphocyte with minor modifications (Kamata et al., 2000). After collagenase procedure, collected cells were placed on a 50% discontinuous Percoll gradient (Sigma) and centrifuged for 20 min at 700× g. A low-density fraction was collected and washed twice. The washed cells were incubated in culture dishes at 37°C for 1 hr to remove adherent cells, and the nonadherent cells were collected. DCs ($CD11c^+$) were isolated from these nonadherent cells with the use of magnetic-antibody cell sorting (MACS) (Miltenyi Biotec). B cells ($B220^+$) and T cells ($CD4^+$ or $CD8^+$) were isolated from the cell suspension of erythrocyte-depleted splenocyte with the use of MACS.

Sequence of PCR Primers

The sequence of PCR primers is provided as supplemental data at http://www.immunity.com/cgi/content/full/18/2/301/DC1.

Acknowledgments

We are grateful to Drs. J. Gyuris, M. Hooper, and S. Itohara for providing critical reagents, Drs. I. Ogawa, A. Mizoguchi, J. Hatakeyama, and R. Kageyama for teaching experimental procedures and, Drs. K. Ikuta and S. Fagarasan for their helpful discussions and critical reading of the manuscript. We also thank Mses. Y. Doi, T. Taniuchi, T. Toyoshima, E. Inoue, A. Nakano, and Y. Tabuchi for their technical assistance, and Mses. T. Nishikawa and Y. Shiraki for help with manuscript preparation. This work was supported by a Center for Excellence grant from the Ministry of Education, Science, Sports and Culture of Japan.

Received: July 26, 2002
Revised: January 9, 2003

References

Apelqvist, A., Li, H., Sommer, L., Beatus, P., Anderson, D.J., Honjo, T., Hrabe de Angelis, M., Lendahl, U., and Edlund, H. (1999). Notch signalling controls pancreatic cell differentiation. Nature *400*, 877–881.

Artavanis-Tsakonas, S., Matsuno, K., and Fortini, M.E. (1995). Notch signaling. Science *268*, 225–232.

Artavanis-Tsakonas, S., Rand, M.D., and Lake, R.J. (1999). Notch signaling: cell fate control and signal integration in development. Science *284*, 770–776.

Bang, A.G., and Posakony, J.W. (1992). The Drosophila gene Hairless encodes a novel basic protein that controls alternative cell fates in adult sensory organ development. Genes Dev. *6*, 1752–1769.

Bang, A.G., Bailey, A.M., and Posakony, J.W. (1995). Hairless promotes stable commitment to the sensory organ precursor cell fate by negatively regulating the activity of the Notch signaling pathway. Dev. Biol. *172*, 479–494.

Beatus, P., and Lendahl, U. (1998). Notch and neurogenesis. J. Neurosci. Res. *54*, 125–136.

Braissant, O., Foufelle, F., Scotto, C., Dauca, M., and Wahli, W. (1996). Differential expression of peroxisome proliferator-activated receptors (PPARs): tissue distribution of PPAR-alpha, -beta, and -gamma in the adult rat. Endocrinology *137*, 354–366.

Brou, C., Logeat, F., Lecourtois, M., Vandekerckhove, J., Kourilsky, P., Schweisguth, F., and Israel, A. (1994). Inhibition of the DNA-binding activity of Drosophila suppressor of hairless and of its human homolog, KBF2/RBP-J kappa, by direct protein-protein interaction with Drosophila hairless. Genes Dev. *8*, 2491–2503.

Furukawa, T., Maruyama, S., Kawaichi, M., and Honjo, T. (1992). The *Drosophila* homolog of the immunoglobulin recombination signal-binding protein regulates peripheral nervous system development. Cell *69*, 1191–1197.

Hamada, Y., Kadokawa, Y., Okabe, M., Ikawa, M., Coleman, J.R., and Tsujimoto, Y. (1999). Mutation in ankyrin repeats of the mouse Notch2 gene induces early embryonic lethality. Development *126*, 3415–3424.

Hamaguchi, Y., Yamamoto, Y., Iwanari, H., Maruyama, S., Furukawa, T., Matsunami, N., and Honjo, T. (1992). Biochemical and immunological characterization of the DNA binding protein (RBP-J kappa) to mouse J kappa recombination signal sequence. J. Biochem. (Tokyo) *112*, 314–320.

Han, H., Tanigaki, K., Yamamoto, N., Kuroda, K., Yoshimoto, M., Nakahata, T., Ikuta, K., and Honjo, T. (2002). Inducible gene knockout of transcription factor recombination signal binding protein-J reveals its essential role in T versus B lineage decision. Int. Immunol. *14*, 637–645.

Hsieh, J.J., Zhou, S., Chen, L., Young, D.B., and Hayward, S.D. (1999). CIR, a corepressor linking the DNA binding factor CBF1 to the histone deacetylase complex. Proc. Natl. Acad. Sci. USA *96*, 23–28.

Izon, D.J., Punt, J.A., and Pear, W.S. (2002). Deciphering the role of Notch signaling in lymphopoiesis. Curr. Opin. Immunol. *14*, 192–199.

Jarriault, S., Brou, C., Logeat, F., Schroeter, E.H., Kopan, R., and Israel, A. (1995). Signalling downstream of activated mammalian Notch. Nature *377*, 355–358.

Kamata, T., Nogaki, F., Fagarasan, S., Sakiyama, T., Kobayashi, I., Miyawaki, S., Ikuta, K., Muso, E., Yoshida, H., Sasayama, S., and Honjo, T. (2000). Increased frequency of surface IgA-positive plasma cells in the intestinal lamina propria and decreased IgA excretion in hyper IgA (HIGA) mice, a murine model of IgA nephropathy with hyperserum IgA. J. Immunol. *165*, 1387–1394.

Kao, H.Y., Ordentlich, P., Koyano-Nakagawa, N., Tang, Z., Downes, M., Kintner, C.R., Evans, R.M., and Kadesch, T. (1998). A histone deacetylase corepressor complex regulates the Notch signal transduction pathway. Genes Dev. *12*, 2269–2277.

Kato, H., Sakai, T., Tamura, K., Minoguchi, S., Shirayoshi, Y., Hamada, Y., Tsujimoto, Y., and Honjo, T. (1996). Functional conservation of mouse Notch receptor family members. FEBS Lett. *395*, 221–224.

Kato, H., Taniguchi, Y., Kurooka, H., Minoguchi, S., Sakai, T., Nomura-Okazaki, S., Tamura, K., and Honjo, T. (1997). Involvement of RBP-J in biological functions of mouse Notch1 and its derivatives. Development *124*, 4133–4141.

Kopan, R., Nye, J.S., and Weintraub, H. (1994). The intracellular domain of mouse Notch: a constitutively activated repressor of myogenesis directed at the basic helix-loop-helix region of MyoD. Development *120*, 2385–2396.

Kuang, B., Wu, S.C., Shin, Y., Luo, L., and Kolodziej, P. (2000). split ends encodes large nuclear proteins that regulate neuronal cell fate and axon extension in the Drosophila embryo. Development *127*, 1517–1529.

Kuroda, K., Tani, S., Tamura, K., Minoguchi, S., Kurooka, H., and Honjo, T. (1999). Delta-induced Notch signaling mediated by RBP-J inhibits MyoD expression and myogenesis. J. Biol. Chem. *274*, 7238–7244.

Kurooka, H., and Honjo, T. (2000). Functional interaction between the mouse notch1 intracellular region and histone acetyltransferases PCAF and GCN5. J. Biol. Chem. *275*, 17211–17220.

Kurooka, H., Kuroda, K., and Honjo, T. (1998). Roles of the ankyrin repeats and C-terminal region of the mouse notch1 intracellular region. Nucleic Acids Res. *26*, 5448–5455.

Lardelli, M., and Lendahl, U. (1993). Motch A and motch B—two mouse Notch homologues coexpressed in a wide variety of tissues. Exp. Cell Res. *204*, 364–372.

Lardelli, M., Dahlstrand, J., and Lendahl, U. (1994). The novel Notch homologue mouse Notch 3 lacks specific epidermal growth factor-repeats and is expressed in proliferating neuroepithelium. Mech. Dev. *46*, 123–136.

Loder, F., Mutschler, B., Ray, R.J., Paige, C.J., Sideras, P., Torres, R., Lamers, M.C., and Carsetti, R. (1999). B cell development in the spleen takes place in discrete steps and is determined by the quality of B cell receptor-derived signals. J. Exp. Med. *190*, 75–89.

Martin, F., and Kearney, J.F. (2001). B1 cells: similarities and differences with other B cell subsets. Curr. Opin. Immunol. *13*, 195–201.

McCright, B., Gao, X., Shen, L., Lozier, J., Lan, Y., Maguire, M., Herzlinger, D., Weinmaster, G., Jiang, R., and Gridley, T. (2001). Defects in development of the kidney, heart and eye vasculature in mice homozygous for a hypomorphic Notch2 mutation. Development *128*, 491–502.

Minoguchi, S., Taniguchi, Y., Kato, H., Okazaki, T., Strobl, L.J., Zimber Strobl, U., Bornkamm, G.W., and Honjo, T. (1997). RBP-L, a transcription factor related to RBP-Jkappa. Mol. Cell. Biol. *17*, 2679–2687.

Mizushima, S., and Nagata, S. (1990). pEF-BOS, a powerful mammalian expression vector. Nucleic Acids Res. *18*, 5322.

Mizutani, T., Taniguchi, Y., Aoki, T., Hashimoto, N., and Honjo, T. (2001). Conservation of the biochemical mechanisms of signal transduction among mammalian Notch family members. Proc. Natl. Acad. Sci. USA *98*, 9026–9031.

Morel, V., Lecourtois, M., Massiani, O., Maier, D., Preiss, A., and Schweisguth, F. (2001). Transcriptional repression by suppressor of hairless involves the binding of a hairless-dCtBP complex in *Drosophila*. Curr. Biol. *11*, 789–792.

Mumm, J.S., Schroeter, E.H., Saxena, M.T., Griesemer, A., Tian, X., Pan, D.J., Ray, W.J., and Kopan, R. (2000). A ligand-induced extracellular cleavage regulates γ-secretase-like proteolytic activation of Notch1. Mol. Cell *5*, 197–206.

Newberry, E.P., Latifi, T., and Towler, D.A. (1999). The RRM domain of MINT, a novel Msx2 binding protein, recognizes and regulates the rat osteocalcin promoter. Biochemistry *38*, 10678–10690.

Ohtsuka, T., Ishibashi, M., Gradwohl, G., Nakanishi, S., Guillemot, F., and Kageyama, R. (1999). Hes1 and Hes5 as notch effectors in mammalian neuronal differentiation. EMBO J. *18*, 2196–2207.

Oliver, A.M., Martin, F., Gartland, G.L., Carter, R.H., and Kearney, J.F. (1997). Marginal zone B cells exhibit unique activation, proliferative and immunoglobulin secretory responses. Eur. J. Immunol. *27*, 2366–2374.

Oswald, F., Kostezka, U., Astrahantseff, K., Bourteele, S., Dillinger, K., Zechner, U., Ludwig, L., Wilda, M., Hameister, H., Knochel, W., et al. (2002). SHARP is a novel component of the Notch/RBP-Jkappa signalling pathway. EMBO J. *21*, 5417–5426.

Radtke, F., Ferrero, I., Wilson, A., Lees, R., Aguet, M., and MacDonald, H.R. (2000). Notch1 deficiency dissociates the intrathymic development of dendritic cells and T cells. J. Exp. Med. *191*, 1085–1094.

Rebay, I., Chen, F., Hsiao, F., Kolodziej, P.A., Kuang, B.H., Laverty, T., Suh, C., Voas, M., Williams, A., and Rubin, G.M. (2000). A genetic screen for novel components of the Ras/Mitogen-activated protein kinase signaling pathway that interact with the yan gene of Drosophila identifies split ends, a new RNA recognition motif-containing protein. Genetics *154*, 695–712.

Schroeter, E.H., Kisslinger, J.A., and Kopan, R. (1998). Notch-1 signalling requires ligand-induced proteolytic release of intracellular domain. Nature *393*, 382–386.

Schweisguth, F., and Posakony, J.W. (1992). Suppressor of Hairless, the *Drosophila* homolog of the mouse recombination signal-binding protein gene, controls sensory organ cell fates. Cell *69*, 1199–1212.

Shi, Y., Downes, M., Xie, W., Kao, H.Y., Ordentlich, P., Tsai, C.C., Hon, M., and Evans, R.M. (2001). Sharp, an inducible cofactor that integrates nuclear receptor repression and activation. Genes Dev. *15*, 1140–1151.

Shinkai, Y., Rathbun, G., Lam, K.P., Oltz, E.M., Stewart, V., Mendelsohn, M., Charron, J., Datta, M., Young, F., Stall, A.M., et al. (1992). RAG-2-deficient mice lack mature lymphocytes owing to inability to initiate V(D)J rearrangement. Cell *68*, 855–867.

Steinman, R.M., Pack, M., and Inaba, K. (1997). Dendritic cells in the T-cell areas of lymphoid organs. Immunol. Rev. *156*, 25–37.

Struhl, G., and Adachi, A. (1998). Nuclear access and action of notch in vivo. Cell *93*, 649–660.

Takebayashi, K., Sasai, Y., Sakai, Y., Watanabe, T., Nakanishi, S., and Kageyama, R. (1994). Structure, chromosomal locus, and promoter analysis of the gene encoding the mouse helix-loop-helix factor HES-1. Negative autoregulation through the multiple N box elements. J. Biol. Chem. *269*, 5150–5156.

Tamura, K., Taniguchi, Y., Minoguchi, S., Sakai, T., Tun, T., Furukawa, T., and Honjo, T. (1995). Physical interaction between a novel domain of the receptor Notch and the transcription factor RBP-J kappa/Su(H). Curr. Biol. *5*, 1416–1423.

Tanigaki, K., Han, H., Yamamoto, N., Tashiro, K., Ikegawa, M., Kuroda, K., Suzuki, A., Nakano, T., and Honjo, T. (2002). Notch-RBP-J signaling is involved in cell fate determination of marginal zone B cells. Nat. Immunol. *3*, 443–450.

Taniguchi, Y., Furukawa, T., Tun, T., Han, H., and Honjo, T. (1998). LIM protein KyoT2 negatively regulates transcription by association with the RBP-J DNA-binding protein. Mol. Cell. Biol. *18*, 644–654.

Uyttendaele, H., Marazzi, G., Wu, G., Yan, Q., Sassoon, D., and Kitajewski, J. (1996). Notch4/int-3, a mammary proto-oncogene, is an endothelial cell-specific mammalian Notch gene. Development *122*, 2251–2259.

Wiellette, E.L., Harding, K.W., Mace, K.A., Ronshaugen, M.R., Wang, F.Y., and McGinnis, W. (1999). spen encodes an RNP motif protein that interacts with Hox pathways to repress the development of head-like sclerites in the Drosophila trunk. Development *126*, 5373–5385.

Yamaguchi, E., Chiba, S., Kumano, K., Kunisato, A., Takahashi, T., and Hirai, H. (2002). Expression of Notch ligands, Jagged1, 2 and Delta1 in antigen presenting cells in mice. Immunol. Lett. *81*, 59–64.

Zhou, S., and Hayward, S.D. (2001). Nuclear localization of cbf1 is regulated by interactions with the smrt corepressor complex. Mol. Cell. Biol. *21*, 6222–6232.